

## Raman scattering on intrinsic surface electron accumulation of InN nanowires

K. Jeganathan, V. Purushothaman, R. K. Debnath, R. Calarco, and H. Luth

Citation: [Applied Physics Letters](#) **97**, 093104 (2010); doi: 10.1063/1.3483758

View online: <http://dx.doi.org/10.1063/1.3483758>

View Table of Contents: <http://scitation.aip.org/content/aip/journal/apl/97/9?ver=pdfcov>

Published by the [AIP Publishing](#)

---

### Articles you may be interested in

[Probing the electron density in undoped, Si-doped, and Mg-doped InN nanowires by means of Raman scattering](#)

Appl. Phys. Lett. **97**, 221906 (2010); 10.1063/1.3520643

[Lineshape analysis of Raman scattering from LO and SO phonons in III-V nanowires](#)

J. Appl. Phys. **106**, 114317 (2009); 10.1063/1.3267488

[Surface optical Raman modes in InN nanostructures](#)

Appl. Phys. Lett. **93**, 233116 (2008); 10.1063/1.3040681

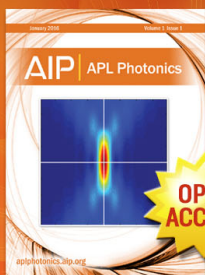
[Structural characterization of GaAs and InAs nanowires by means of Raman spectroscopy](#)

J. Appl. Phys. **104**, 104311 (2008); 10.1063/1.3026726

[Raman scattering in InAs nanowires synthesized by a solvothermal route](#)

Appl. Phys. Lett. **89**, 253117 (2006); 10.1063/1.2422897

---



Launching in 2016!  
The future of applied photonics research is here

**AIP** | APL  
Photonics

# Raman scattering on intrinsic surface electron accumulation of InN nanowires

K. Jeganathan,<sup>1,a)</sup> V. Purushothaman,<sup>1</sup> R. K. Debnath,<sup>2</sup> R. Calarco,<sup>3</sup> and H. Luth<sup>3</sup>

<sup>1</sup>Centre for Nanoscience and Nanotechnology, School of Physics, Bharathidasan University, Tiruchirappalli 620 024, India

<sup>2</sup>Department of Electrical and Computer Engineering, University of Toronto, 10 King's College Road, Toronto, Ontario M5S 3G4, Canada

<sup>3</sup>Institute of Bio- and Nanosystems (IBN-1), Research Centre Jülich GmbH, D-52425 Jülich, Germany

(Received 18 May 2010; accepted 1 August 2010; published online 1 September 2010)

An intrinsic property of vertically aligned InN nanowire (NW) ensembles have been investigated by analysis of coupled longitudinal optical (LO) phonon mode using  $\mu$ -Raman scattering. Spectra were recorded in backscattering geometries in parallel and perpendicular to the axis of the NWs. The width of surface accumulation layer is estimated from the LO phonon peak intensity ratios. The carrier concentration is extracted to be  $6.7 \times 10^{16} \text{ cm}^{-3}$ . The pronounced peak at  $627.2 \text{ cm}^{-1}$  is related to the interaction of phonons with surface electrons. The surface charge density,  $N_{sc}$  is calculated to be  $\sim 2.55 \times 10^{13} \text{ cm}^{-2}$  which provides surface accumulation field strength of  $5.5 \text{ Mv/cm}$ . © 2010 American Institute of Physics. [doi:10.1063/1.3483758]

Indium Nitride (InN), the least studied among III-Nitrides, has received a substantial interest because of its revised narrow band gap<sup>1,2</sup> (0.65–0.7 eV) and excellent electrical properties.<sup>3,4</sup> Despite the number of fundamental difficulties such as low dissociation temperature, weak In–N bonding and high equilibrium pressure of  $N_2$ , the recent advances in the synthesis of low dimensional InN nanowires (NWs) by plasma-assisted molecular beam epitaxy (MBE) provides an ideal platform to study the intrinsic properties of InN.<sup>5,6</sup> The accumulation layer at the surface of InN and high surface-to-volume ratio renders them excellent candidates for near infrared emission<sup>5–7</sup> and sensing devices.<sup>8,9</sup> The electron accumulation at the surface of InN is formed due to the existence of occupied surface states at the conduction-band-minimum.<sup>10</sup> The width of the accumulation is reported to be  $\sim 3 \text{ nm}$  with high charge sheet density ( $\sim 10^{13} \text{ cm}^{-2}$ ). The presence of electron accumulation at the surface complicates the measurements of electrical properties of bulk InN.<sup>11</sup> It is expected to interfere with the true bulk properties which may result wide experimental error in the determination of carrier concentration. It is unlikely to exclude the influence of surface accumulation in the single field Hall measurements, thus the determination of carrier concentration of InN and the surface accumulation layer is uncertain. On the other hand, simple contact-less and non-destructive Raman scattering provides an ideal probe to distinguish bulk and surface properties of degenerate semiconductors.<sup>12–14</sup>

In general, if the penetration depth is larger than the width of surface accumulation layer, Raman spectra should be expected to show both the bands of coupled LO phonon from bulk ( $\omega_{LO}$ ) and surface electron induced LO ( $\omega_{SLO}$ ) phonon at higher frequencies. The intensity of the LO phonon from bulk has been shown to highly depend on the width of the surface accumulation and penetration depth of the excitation wavelength.<sup>12–14</sup> Further, as the increase in carrier

levels the width of the surface accumulation reaches minimum values. The intensity of LO phonon  $I(LO)$  under the influence of surface accumulation can be written as<sup>14</sup>

$$I(LO) = I_0(LO)[1 - \exp(-2w_s/d)], \quad (1)$$

where  $I_0(LO)$  is the intensity of LO phonon observed in a low carrier concentration sample and  $d$  is the optical skin depth. The width of the surface accumulation ( $w_s$ ), can easily be estimated from the peak intensity ratio of  $A_1(LO)$  modes.

The aim of this letter is to investigate the intrinsic properties of InN, in particular, thickness of surface accumulation and bulk carrier densities.

Self-assembled InN NWs were fabricated by plasma-assisted MBE on Si (111) substrates.<sup>5,6</sup>  $\mu$ -Raman scattering measurements were performed in backscattering geometry using Dilor-LabRam Raman spectrometer with a resolution of  $0.3 \text{ cm}^{-1}$ . The wavelength of  $514.5 \text{ nm}$  line of Ar-ion laser was used as an excitation source and the laser beam was focused through a microscope (100 $\times$ , numerical aperture 0.9) with a spot size of about  $1 \text{ }\mu\text{m}$  in diameter. The typical laser power at the surface of wire was  $0.25 \text{ mW}$ . A liquid nitrogen cooled charge coupled device was used to collect the scattered signal dispersed on 1800 grooves/mm grating. The backscattering Raman spectra were recorded in two different directions in one which the as-grown vertical aligned InN NWs on Si (111) where c-axis (0001) of the wire is parallel to the laser beam and the other on the C-axis of the wire perpendicular to the incident beam. Obviously, the NWs are cylindrically (optically) symmetric. Hence, Raman spectra of bulk phonon modes are expected to be independent of scattering direction. As the NWs are optically symmetric and the diameter ( $\sim 150 \text{ nm}$ ) is much smaller than the wavelength of the excitation light, the internal field in NWs may be polarized perpendicular to the NW axes and attenuated with respect to external field. The damping factor highly depends on the dielectric constant of InN ( $\epsilon$ ) and surrounding medium ( $\epsilon_0$ ). The attenuation factor considering the dielectric medium may forbid the selection rules for Raman Scat-

<sup>a)</sup>Author to whom correspondence should be addressed. Electronic mail: k.jeganathan@yahoo.com.

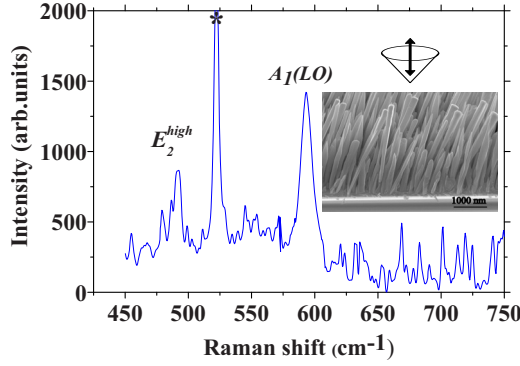


FIG. 1. (Color online) Raman spectra of as-grown vertical aligned InN NW recorded in backscattering geometry parallel to the c-axis for excitation laser power of 0.25 mW near the sample surface. Silicon peak is marked by an asterisk (\*).

tering and the scattering modes intensity can be reduced due to anisotropy on the surface of the NWs.

The first-order Raman spectrum of InN NWs measured along the c-axis parallel to the laser beam in backscattering  $z(-,-)\bar{z}$  geometry is shown in Figure 1. The inset shows the field emission scanning electron micrograph of as-grown InN NWs and its scattering direction. Two well resolved active phonon modes are observed at 491 and 594  $\text{cm}^{-1}$ , pertaining to  $E_2(\text{high})$  and  $A_1(\text{LO})$  phonon of InN, respectively.

A sharp full-width at half maximum of 4.7  $\text{cm}^{-1}$  for  $E_2(\text{high})$  phonon and its peak position close to the reported values attributes good crystalline quality and higher degrees of relaxation. The integrated intensity of  $E_2(\text{high})$  phonon is much lower than that of  $A_1(\text{LO})$  mode, however, any direct relationship between nonpolar  $E_2(\text{high})$  and polar  $A_1(\text{LO})$  mode could not be established as due to noninteraction of  $E_2(\text{high})$  with surface electrons and should be expected that the frequency, intensity and broadening of this mode remain unchanged by the scattering geometry. Nevertheless, the polar  $A_1(\text{LO})$  mode is expected to interact with plasmons or surface electrons. Hence, the behavior of this  $A_1(\text{LO})$  structure is particularly intriguing due to surface accumulated electrons and interpretation become more difficult and challenging. The LO phonon-like structure had been observed in InN layers with a wide range of carrier densities and this peak gains intensity as well as broaden asymmetrically with increasing carrier concentration but the peak position remain within the range of 580–596  $\text{cm}^{-1}$ .<sup>15,16</sup> The theoretical approach on the interaction of phonon with plasmon results two coupled modes. However, the frequency of the experimentally observed peaks did not match with the theoretically calculated coupled modes.<sup>15</sup> It has never been observed higher energy mode of the coupled phonon-plasmon peak as a substantial shift in  $A_1(\text{LO})$  mode.<sup>15,16</sup> But, the lower branch of coupled LO mode has been reported to disperse and approach the frequency of TO phonon mode as the increase in carrier concentration. This anomalous behavior was explained by the scattering of structural defects induced electron-hole pairs with LO phonon.<sup>16</sup> But the discussion on the interaction of phonons with the surface accumulation of electron is completely absent.<sup>15,16</sup>

The optical absorption coefficient ( $\alpha$ ) of InN for 2.41 eV excitation energy is  $\sim 1.2 \times 10^5 \text{ cm}^{-1}$ . The optical skin depth ( $d = 1/2\alpha$ ) is inversely proportional to the excitation

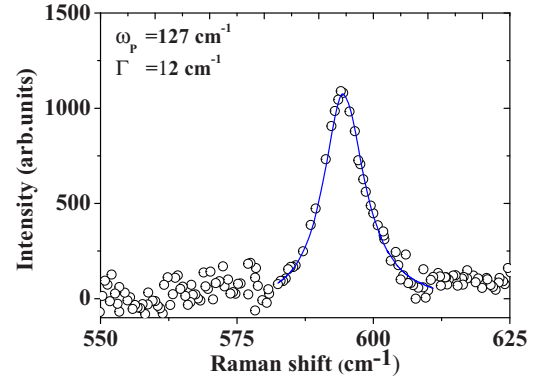


FIG. 2. (Color online) Raman spectrum of coupled LO phonon-plasmon mode of InN nanowires.

energy,<sup>17</sup> in this case minimum probe depth would be expected for InN excited with the phonon energy of 2.41 eV. This corresponds to an optical skin depth of  $\sim 41 \text{ nm}$ , which is about several times the width of the surface accumulation layer. No additional peak related to surface accumulation was observed in the scattering vector parallel to the c-axis (Fig. 1). Nevertheless, the coupling of LO phonon with plasmon free carriers are not ruled out on the basis of an observation of low energy coupled LO phonon modes.<sup>16</sup>

The displayed  $A_1(\text{LO})$  mode can be intimately related to the coupled mode and its intensity profile is expressed as a function of deformation potential and electro-optic mechanism<sup>18,19</sup>

$$I_A = SA(\omega)\text{Im}\left[-\frac{1}{\varepsilon(\omega)}\right], \quad (2)$$

where  $\omega$  is the Raman shift,  $\varepsilon(\omega)$  is the dielectric function and parameter  $A(\omega)$  can be found elsewhere.<sup>18</sup> The line shape of the coupled mode was fitted with the function given in Eq. (2). The dielectric  $\varepsilon(\omega)$  and phonon contribution  $A(\omega)$  are function of plasmon damping constant ( $\gamma$ ), phonon damping ( $\Gamma$ ), and plasmon frequency ( $\omega_p$ ) parameters. The proportionality constant,  $S$  is treated as an independent of carrier concentration. The frequency of the unscreened  $\omega_{\text{LO}} = 590 \text{ cm}^{-1}$  from the theoretical calculations on InN and  $\omega_{\text{TO}} = \omega_{\text{LO}}\sqrt{\varepsilon_\infty/\varepsilon_0}$  from Lyddane–Sachs–Teller relation, are used for this line fitting. Here, we use the dielectric constants  $\varepsilon_\infty = 8.4$ ,  $\varepsilon_0 = 15.3$  and Faust–Henry coefficient  $C$  ( $-2.0$ ) for this fitting. A careful attention has been paid for the baseline correction of the experimental curve.

Figure 2 shows a typical line shape of the experimental (open circle) and the theoretical fitted curve (solid line) of the coupled  $A_1(\text{LO})$  mode. The reproducible fitting parameters  $\Gamma$  and  $\omega_p$  have been obtained from the above line shape analysis.<sup>20</sup> The plasmon frequency  $\omega_p$  can be related to the free carriers ( $n$ ) and effective electron mass of InN (Refs. 19 and 21) ( $m^* = 0.07m_e$ ),

$$\omega_p^2 = \frac{\pi n e^2}{\varepsilon_\infty m^*}. \quad (3)$$

The electron concentration obtained by line shape analysis is  $6.7 \times 10^{16} \text{ cm}^{-3}$ . It should be noted that the carrier concentration is far below to the reported values of InN compact layer. Because of the low carrier concentration the coupled phonon mode might be very close to the generic  $A_1(\text{LO})$



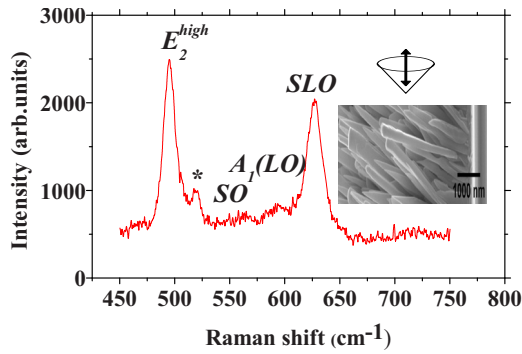


FIG. 3. (Color online) Raman spectra of InN NWs recorded perpendicular to the c-axis of nanowire. Silicon peak is marked by an asterisk (\*).

phonon frequency. The plasmon frequency,  $\omega_p = 127 \text{ cm}^{-1}$ , is lower than the unscreened coupled LO phonon ( $594 \text{ cm}^{-1}$ ) which implies that the character of the coupled mode is phonon-like.

Raman scattering recorded perpendicular to the c-axis of the wires shows an additional peak at  $627.2 \text{ cm}^{-1}$  related to surface accumulation of electrons as shown in Fig. 3. Since the NW axis is perpendicular to the incident laser beam, the scattering geometry is represented by  $x(-,-)\bar{x}$ . The inset shows SEM image of titled c-axis of InN NWs perpendicular to the laser beam. The generic  $A_1(\text{LO})$  phonon peak intensity is very weak but the frequency unchanged by the scattering geometry. Further, emergence of peak at the frequency of the unscreened LO phonon suggested that existence of accumulation layer. Hence, this persistent reduction in intensity can be related to the width of electron accumulation layer. The intensity of  $A_1(\text{LO})$  mode parallel to the c-axis of the wire has been considered as a reference of  $I_0(\text{LO})$  because of low carrier concentration and the absence of surface electron—phonon interaction. From the intensity ratio of  $A_1(\text{LO})$  phonon modes in two different NW direction, width of the surface accumulation was estimated to be  $\sim 8 \text{ nm}$  by employing an empirical formula given in Eq. (1). The electron accumulation width on the surface of NWs is more than twice that of earlier reported values ( $\sim 3 \text{ nm}$ ) of InN compact layers with high carrier concentration. This clearly evidence that the low carrier concentration and high surface area heightens the accumulation of electrons at the surface of InN NWs. An another broad peak is also evident between the  $E_2(\text{high})$  and  $A_1(\text{LO})$  phonon of the spectrum in Fig. 3, is ascribed to be surface mode due to high surface-volume-ratio of NWs. This peak is expected to disperse between TO and LO modes depending on the break in the wave vector ( $\vec{q} = \vec{k}_{\text{inc}} - \vec{k}_{\text{scatt}}$ ) along the surface potential.<sup>21</sup>

The emergence of surface LO (SLO) phonon peak evidences the strong interaction of LO phonons with surface electrons and this can also be substantiated by the weak intensity of  $A_1(\text{LO})$  phonon mode as compared to parallel to the c-axis. The electron-phonon interaction energy  $E_{ep} = \sqrt{2m^* \omega_{\text{SLO}} \hbar}^{-1}$  is calculated to be  $15.4 \text{ meV}$ . The plasmon frequency of this SLO mode,  $\omega_p = 637 \text{ cm}^{-1}$ , is very high as compared to the LO phonon frequency, which means that SLO mode shows a typical behavior of plasmon. The line profile analysis of SLO mode provide information on surface

charge density of electrons from which strength of electron accumulation energy can be estimated. By considering the average diameter of InN NW is  $150 \text{ nm}$ , the surface charge density is estimated to be  $N_{ss} \approx 2.55 \times 10^{13} \text{ cm}^{-2}$  and the corresponding electron accumulation field strength ( $E_D \approx 5.5 \text{ Mv/cm}$ ) at the surface of NWs is very strong. The origin of SLO relative to the surface accumulation can explained by the surface Fermi level pinning high in the conduction band in the vicinity of low  $\Gamma$ -point which produces charge donor-type surface states resulting in downward band bending.<sup>10</sup>

In conclusion, the LO phonon mode in InN NWs investigated by line shape analysis provides a powerful probe of electron surface accumulation layer and also estimation of bulk carrier concentration. The emergence of well-defined SLO peak at higher frequency of generic  $A_1(\text{LO})$  phonon-like reveals the existence of intrinsic electron accumulation layer at the surface of InN NWs. The width of the surface accumulation is  $\sim 8 \text{ nm}$  and its corresponding field strength is found to be  $5.5 \text{ Mv/cm}$ .

The authors wish to thank Mr. K. H. Deussen for technical support. One of the authors (K.J.) gratefully acknowledges the Department of Science and Technology, Govt. of India for partial financial support under research Contract Nos. SR/FTP/PS-64/2007 and SR/NM/NS-77/2008.

- <sup>1</sup>V. Y. Davydov, A. Klochikhin, A. R. P. Seisyan, V. V. Emtsev, S. V. Ivano, S. V. Bechstedt, J. Furthmüller, S. V. Harima, A. V. Mudryi, J. Aderhold, and O. Semchinova, *Phys. Status Solidi B* **229**, r1 (2002).
- <sup>2</sup>J. Wu, W. Walukiewicz, K. M. Yu, J. W. Ager, E. E. Haller, L. Hai, J. S. William, S. Yoshiki, and N. Yasushi, *Appl. Phys. Lett.* **80**, 3967 (2002).
- <sup>3</sup>K. T. Tsen, C. Poweleit, D. K. Ferry, H. Lu, and W. J. Schaff, *Appl. Phys. Lett.* **86**, 222103 (2005).
- <sup>4</sup>S. K. O'Leary, B. E. Foutz, M. S. Shur, and L. F. Eastman, *Appl. Phys. Lett.* **87**, 222103 (2005).
- <sup>5</sup>T. Stoica, R. Meijers, R. Calarco, T. Richter, and H. Luth, *J. Cryst. Growth* **290**, 241 (2006).
- <sup>6</sup>T. Stoica, R. J. Meijers, R. Calarco, T. Richter, E. Sutter, and H. Luth, *Nano Lett.* **6**, 1541 (2006).
- <sup>7</sup>C. H. Shen, H. Y. Chen, H. W. Lin, S. Gwo, A. A. Klochikhin, and V. Y. Davydov, *Appl. Phys. Lett.* **88**, 253104 (2006).
- <sup>8</sup>L. Hai, J. S. William, and F. E. Lester, *J. Appl. Phys.* **96**, 3577 (2004).
- <sup>9</sup>O. Kryliouk, H. J. Park, H. T. Wang, B. S. Kang, T. J. Anderson, F. Ren, and S. J. Pearton, *J. Vac. Sci. Technol. B* **23**, 1891 (2005).
- <sup>10</sup>I. Mahboob, T. D. Veal, C. F. McConville, H. Lu, and W. J. Schaff, *Phys. Rev. Lett.* **92**, 036804 (2004).
- <sup>11</sup>T. D. Veal, I. Mahboob, L. F. J. Piper, C. F. McConville, H. Lu, and W. J. Schaff, *J. Vac. Sci. Technol. B* **22**, 2175 (2004).
- <sup>12</sup>A. Pinczuk and E. Burstein, *Phys. Rev. Lett.* **21**, 1073 (1968).
- <sup>13</sup>P. Corden, A. Pinczuk, and E. Burstein, Proceedings of the 10th International Conference on the Physics of Semiconductors, 1970, p. 739.
- <sup>14</sup>H. Shen, F. H. Pollak, and R. N. Sacks, *Appl. Phys. Lett.* **47**, 891 (1985).
- <sup>15</sup>J. S. Thakur, D. Haddad, V. M. Naik, R. Naik, G. W. Auner, H. Lu, and W. J. Schaff, *Phys. Rev. B* **71**, 115203 (2005).
- <sup>16</sup>V. Y. Davydov and A. A. Klochikhin, *Semiconductors* **38**, 861 (2004).
- <sup>17</sup>H. Ahn, C. H. Shen, C. L. Wu, and S. Gwo, *Appl. Phys. Lett.* **86**, 201905 (2005).
- <sup>18</sup>G. Immer, V. V. Toporov, B. H. Bairamov, and J. Monecke, *Phys. Status Solidi B* **119**, 595 (1983).
- <sup>19</sup>M. V. Klein, B. N. Ganguly, and P. J. Colwell, *Phys. Rev. B* **6**, 2380 (1972).
- <sup>20</sup>H. Harima, *J. Phys.: Condens. Matter* **14**, 967 (2002).
- <sup>21</sup>K. Jeganathan, R. K. Debnath, R. Meijers, T. Stoica, R. Calarco, D. Grütz-macher, and H. Lüth, *J. Appl. Phys.* **105**, 123707 (2009).